DEUTSCHES ELEKTRONEN – SYNCHROTRON

DESY 92-164
November 1992

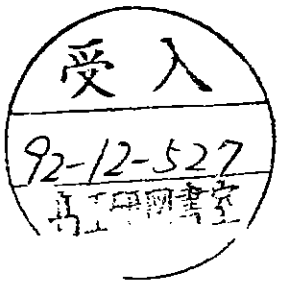

Observation of Deep Inelastic Scattering at Low x

H1 Collaboration

ISSN 0418-9833

NOTKESTRASSE 85 · D-2000 HAMBURG 52

To be sure that your preprints are promptly included in the
HIGH ENERGY PHYSICS INDEX,
send them to (if possible by air mail):

DESY
Bibliothek
Notkestraße 85
W-2000 Hamburg 52
Germany

DESY-IfH
Bibliothek
Platanenallee 6
O-1615 Zeuthen
Germany

DESY 92-164
November 1992

ISSN 0418-9833

Observation of Deep Inelastic Scattering at Low x

H1 Collaboration

Abstract

Measurements of the scattered electron energy spectrum and the differential cross sections $d\sigma/d\log(x)$ and $d\sigma/dQ^2$ for inclusive neutral current deep inelastic electron proton scattering are presented. The data were obtained with the H1 detector at HERA during its first running period in which 26.7 GeV electrons collided with 820 GeV protons. The data correspond to an integrated luminosity of 1.3 nb^{-1} and allow the first studies of the structure of the proton at values of x down to 10^{-4} for $Q^2 > 5$ GeV^2.

Submitted to Physics Letters B, 20 November 1992

Observation of Deep Inelastic Scattering at I

H1 Collaboration

T. Ahmed[3], V. Andreev[22], B. Andrieu[25], M. Arpagaus[32], A. Babaev[21], H. Bärwolff[31], J. Bán[15], P. Baranov[22], E. Barrelet[26], W. Bartel[11], U. Bassler[26], G.A. Beck[17], H.P. B H.-J. Behrend[11], A. Belousov[22], Ch. Berger[1], H. Bergstein[1], G. Bernardi[26], R. Bernet U. Berthon[25], G. Bertrand-Coremans[4], M. Besançon[9], P. Biddulph[20], E. Binder[11], J.C. Bizot[24], V. Blobel[13], K. Borras[8], P.C. Bosetti[2], V. Boudry[25], C. Bourdarios[24], F. Brasse[11], U. Braun[2], W. Braunschweig[1], V. Brisson[24], D. Bruncko[15], J. Bürger[11], F.W. Büsser[13], A. Buniatian[11,35], S. Burke[17], G. Buschhorn[23], A.J. Campbell[10], T. C F. Charles[26], D. Clarke[5], A.B. Clegg[16], M. Colombo[8], J.A. Coughlan[5], A. Courau[24], Ch. Coutures[9], G. Cozzika[9], L. Criegee[11], J. Cvach[25], J.B. Dainton[17], M. Danilov[21], A.W.E. Dann[20], W.D. Dau[14], M. David[9], E. Deffur[11], B. Delcourt[24], L. DelBuono[26], M. Devel[24], A. DeRoeck[11], P. Dingus[25], C. Dollfus[33], J.D. Dowell[3], H B. Dreis[2], A. D J. Duboc[26], D. Düllmann[13], O. Dünger[13], H. Duhm[12], M. Eberle[12], J. Ebert[30], T.R. G. Eckerlin[11], V. Efremenko[21], S. Egli[33], S. Eichenberger[33], R. Eichler[32], F. Eisele[11], E. Eisenhandler[18], N.N. Ellis[3], R.J. Ellison[20], E. Elsen[11], M. Erdmann[11], E. Evrard[4], L. Favart[4], A. Fedotov[21], D. Feeken[13], R. Felst[11], J. Feltesse[9], Y. Feng[26], I.F. Fensom J. Ferencei[11], F. Ferrarotto[29], W. Flauger[11,!], M. Fleischer[11], G. Flügge[2], A. Fomenk B. Fominykh[21], M. Forbush[7], J. Formánek[28], J.M. Foster[20], G. Franke[11], E. Fretwurs P. Fuhrmann[1], E. Gabathuler[17], K. Gamerdinger[23], J. Garvey[3], J. Gayler[11], A. Gellri M. Gennis[11], U. Gensch[31], H. Genzel[1], R. Gerhards[11], D. Gillespie[17], L. Godfrey[7], U. Goerlach[11], L. Goerlich[6], M. Goldberg[26], A.M. Goodall[17], I. Gorelov[21], P. Goritch C. Grab[32], H. Grässler[2], R. Grässler[2], T. Greenshaw[17], H. Greif[23], G. Grindhammer[2 C. Gruber[14], J. Haack[31], D. Haidt[11], L. Hajduk[6], O. Hamon[26], D. Handschuh[11], E.M. Hanlon[16], M. Hapke[11], J. Harjes[13], P. Hartz[8], R. Haydar[24], W.J. Haynes[5], J. Heatherington[18], V. Hedberg[19], R. Hedgecock[5], G. Heinzelmann[13], R.C.W. Hender H. Henschel[31], R. Herma[1], I. Herynek[27], W. Hildesheim[26], P. Hill[11], C.D. Hilton[20], J. Hladký[27], K.C. Hoeger[20], Ph. Huet[4], H. Hufnagel[8], N. Huot[26], M. Ibbotson[20], M.A A. Jacholkowska[24], C. Jacobsson[19], M. Jaffre[24], L. Jönsson[19], K. Johannsen[13], D.P. J L. Johnson[16], H. Jung[2], P.I.P. Kalmus[18], S. Kasarian[11], R. Kaschowitz[2], P. Kasselma U. Kathage[14], H. H.Kaufmann[31], I.R. Kenyon[3], S. Kermiche[24], C. Kiesling[23], M. Klei C. Kleinwort[13], G. Knies[11], T. Köhler[1], H. Kolanoski[8], F. Kole[7], S.D. Kolya[20], V. Ko M. Korn[8], P. Kostka[31], S.K. Kotelnikov[22], M.W. Krasny[6,9], H. Krehbiel[11], D. Krücke U. Krüger[11], J.P. Kubenka[23], H. Küster[11], M. Kuhlen[23], T. Kurča[15], J. Kurzhöfer[8], B. Kuznik[30], R. Lander[7], M.P.J. Landon[18], R. Langkau[12], P. Lanius[23], J.F. Laporte[9], A. Lebedev[22], A. Leuschner[11], C. Leverenz[11], D. Levin[11], S. Levonian[11,22], Ch. Ley[2], A. Lindner[8], G. Lindström[12], P. Loch[11], H. Lohmander[19], G.C. Lopez[18], D. Lüers[23,!], N. Magnussen[30], E. Malinovski[22], S. Mani[7], P. Marage[4], J. Marks[10], R. Marshall[20], J. Martens[30], R. Martin[17], H.-U. Martyn[1], J. Martyniak[6], S. Masson[2], A. Mavroidis[16] S.J. Maxfield[17], S.J. McMahon[17], A. Mehta[20], K. Meier[11], T. Merz[11], C.A. Meyer[33], H. Meyer[30], J. Meyer[11], S. Mikocki[6,24], V. Milone[29], E. Monnier[26], F. Moreau[25], J. M J.V. Morris[5], J.M. Morton[17], K. Müller[33], P. Murín[15], S.A. Murray[20], V. Nagovizin[21], B. Naroska[13], Th. Naumann[31], D. Newton[16], H.K. Nguyen[26], F. Niebergall[13], R. Nisiu G. Nowak[6], G.W. Noyes[3], M. Nyberg[19], H. Oberlack[23], U. Obrock[8], J.E. Olsson[11], S. Orenstein[25], F. Ould-Saada[13], C. Pascaud[24], G.D. Patel[17], E. Peppel[11], S. Peters[23] H.T. Phillips[3], J.P. Phillips[20], Ch. Pichler[12], W. Pilgram[2], D. Pitzl[32], R. Prosi[11], F. R K. Rauschnabel[8], P. Reimer[27], P. Ribarics[23], V. Riech[12], J. Riedlberger[32], M. Rietz[2],

S.M. Robertson[3], P. Robmann[33], R. Roosen[4], A. Rostovtsev[21], C. Royon[9], M. Rudowicz[23], M. Ruffer[12], S. Rusakov[22], K. Rybicki[6], E. Ryseck[31], J. Sacton[4], N. Sahlmann[2], E. Sanchez[23], D.P.C. Sankey[5], M. Savitsky[11], P. Schacht[23], P. Schleper[1], W. von Schlippe[16], C. Schmidt[11], D. Schmidt[30], W. Schmitz[2], V. Schröder[11], M. Schulz[11], A. Schwind[31], W. Scobel[12], U. Seehausen[13], R. Sell[11], M. Seman[15], A. Semenov[21], V. Shekelyan[21], I. Sheviakov[22], H. Shooshtari[29], G. Siegmon[14], U. Siewert[14], Y. Sirois[25], I.O. Skillicorn[10], P. Smirnov[22], J.R. Smith[7], L. Smolik[11], Y. Soloviev[22], H. Spitzer[13], P. Staroba[27], M. Steenbock[13], P. Steffen[11], R. Steinberg[2], H. Steiner[26], B. Stella[29], K. Stephens[20], J. Stier[11], J. Strachota[11], U. Straumann[33], W. Struczinski[2], J.P. Sutton[20], R.E. Taylor[34,24], G. Thompson[18], R.J. Thompson[20], I. Tichomirov[21], C. Trenkel[14], P. Truöl[33], V. Tchernyshov[21], J. Turnau[6], J. Tutas[1], L. Urban[23], A. Usik[22], S. Valkar[28], A. Valkarova[28], C. Vallee[26], P. VanEsch[4], A. Vartapetian[11,35], Y. Vazdik[22], M. Vecko[27], P. Verrecchia[9], R. Vick[13], G. Villet[9], E. Vogel[1], K. Wacker[8], I.W. Walker[16], A. Walther[8], G. Weber[13], D. Wegener[8], A. Wegner[11], H. P.Wellisch[23], S. Willard[7], M. Winde[31], G.-G. Winter[11], Th. Wolff[32], L.A. Womersley[17], A.E. Wright[20], N. Wulff[11], T.P. Yiou[26], J. Žáček[24,28], P. Závada[27], C. Zeitnitz[12], H. Ziaeepour[24], M. Zimmer[11], W. Zimmermann[11], and F. Zomer[24]

[1] *I. Physikalisches Institut der RWTH, Aachen, Germany*[a]
[2] *III. Physikalisches Institut der RWTH, Aachen, Germany*[a]
[3] *School of Physics and Space Research, University of Birmingham, Birmingham, UK*[b]
[4] *Inter-University Institute for High Energies ULB-VUB, Brussels, Belgium*[c]
[5] *Rutherford Appleton Laboratory, Chilton, Didcot, UK*[b]
[6] *Institute for Nuclear Physics, Cracow, Poland*
[7] *Physics Department and IIRPA, University of California, Davis, California, USA*[d]
[8] *Institut für Physik, Universität Dortmund, Dortmund, Germany*[a]
[9] *DAPNIA, Centre d'Etudes de Saclay, Gif-sur-Yvette, France*
[10] *Department of Physics and Astronomy, University of Glasgow, Glasgow, UK*[b]
[11] *DESY, Hamburg, Germany*[a]
[12] *I. Institut für Experimentalphysik, Universität Hamburg, Hamburg, Germany*[a]
[13] *II. Institut für Experimentalphysik, Universität Hamburg, Hamburg, Germany*[a]
[14] *Institut für Reine und Angewandte Kernphysik, Universität Kiel, Kiel, Germany*[a]
[15] *Institute of Experimental Physics, Slovak Academy of Sciences, Kosice, CSFR*
[16] *School of Physics and Materials, University of Lancaster, Lancaster, UK*[b]
[17] *Department of Physics, University of Liverpool, Liverpool, UK*[b]
[18] *Queen Mary and Westfield College, London, UK*[b]
[19] *Physics Department, University of Lund, Lund, Sweden*[e]
[20] *Physics Department, University of Manchester, Manchester, UK*[b]
[21] *Institute for Theoretical and Experimental Physics, Moscow, Russia*
[22] *Lebedev Physical Institute, Moscow, Russia*
[23] *Max-Planck-Institut für Physik, München, Germany*[a]
[24] *LAL, Université de Paris-Sud, IN2P3-CNRS, Orsay, France*
[25] *LPNHE, Ecole Polytechnique, IN2P3-CNRS, Palaiseau, France*
[26] *LPNHE, Universités Paris VI and VII, IN2P3-CNRS, Paris, France*
[27] *Institute of Physics, Czechoslovak Academy of Sciences, Praha, CSFR*
[28] *Nuclear Center, Charles University, Praha, CSFR*
[29] *INFN Roma and Dipartimento di Fisica, Universita "La Sapienzia", Roma, Italy*
[30] *Fachbereich Physik, Bergische Universität Gesamthochschule Wuppertal, Wuppertal, Germany*[a]
[31] *DESY, Institut für Hochenergiephysik, Zeuthen, Germany*[a]
[32] *Institut für Mittelenergiephysik, ETH, Zürich, Switzerland*[f]
[33] *Physik-Institut der Universität Zürich, Zürich, Switzerland*[f]
[34] *Stanford Linear Accelerator Center, Stanford California, USA*
[35] *Visitor from Yerevan Phys.Inst., Armenia*
[†] *Deceased*

[a] *Supported by the Bundesministerium für Forschung und Technologie, F*
[b] *Supported by the UK Science and Engineering Research Council*
[c] *Supported by IISN-IIKW, NATO CRG-890178*
[d] *Supported in part by USDOE grant DE F603 91ER40674*
[e] *Supported by the Swedish Natural Science Research Council*
[f] *Supported by the Swiss National Science Foundation*

1 Introduction

Since the discovery of partons more than 20 years ago[1], deep inelastic lepton scattering experiments [2,3] have provided important information on the structure of the proton and on the nature of the interactions between leptons and quarks. The electron proton collider HERA allows the extension of this line of research into as yet unexplored kinematic regions.

This paper describes the analysis of data taken with the H1 detector [4,5] in July of 1992, HERA's first running period. Both the H1 and ZEUS experiments have presented preliminary results from this period [4,6].

The kinematics of the inclusive deep inelastic scattering (DIS) process $ep \to eX$ is determined by two independent variables, conventionally chosen to be two of x, y and Q^2. These variables may be measured using information from either the scattered lepton or the hadronic system or both. The polar angle θ_e of the scattered electron is measured relative to the proton beam direction, termed the forward direction in the following. The angle, θ_e, and the energy of the scattered lepton, E'_e, determine the above variables through the relations

$$Q^2 = 4E_eE'_e\cos^2(\theta_e/2), \quad y = 1-(E'_e/E_e)\sin^2(\theta_e/2) \text{ and } x = Q^2/(sy), \qquad (1)$$

where the centre of mass energy squared $s = 4E_eE_p = 87\,600$ GeV^2, and E_e and E_p are the energies of the incoming electron and proton, respectively. Due to the large centre of mass energy, x values down to $\sim 10^{-4}$ can be studied in the deep inelastic regime. A salient feature of the kinematics is a peak in the scattered electron energy spectrum at the beam energy E_e for electrons scattered into the backward region $\theta_e > 150°$. This peak, termed the kinematic peak in the following, is of particular interest for calibration purposes. The outgoing hadrons are used for a complementary determination of y using the relation[7]

$$y_h = \sum_{hadrons} \frac{(E_h - p_{z,h})}{2E_e}, \qquad (2)$$

where the E_h are the energies of the hadrons and the p_z their momenta in the z or proton beam direction.

At HERA the electroweak interaction rate is orders of magnitude smaller than the background rate caused by strong interactions of beam protons with either the residual gas in the beampipe or with the material of the beampipe itself. Moreover, at low scattered electron energies, the background rate due to photoproduction events is much larger than the rate of deep inelastic events. The identification of the deep inelastic events is discussed in detail in the following. The data sample is used to derive a first measurement of the neutral current cross section in the new kinematic range.

2 The H1 Detector

Fig. 1 shows a deep inelastic scattering event at $x = 0.002$ and $Q^2 = 17$ GeV^2 observed in the H1 detector. Most of the detector components important for this analysis are visible. These are:

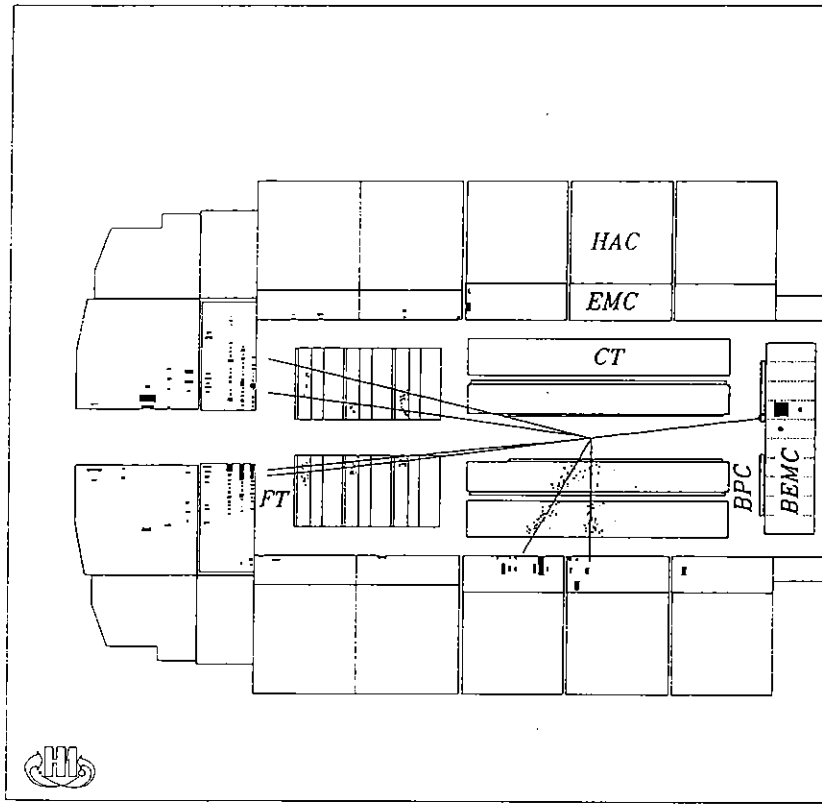

Figure 1: A deep inelastic scattering event at $x = 0.002$ and $Q^2 = 17$ GeV^2, obse
in the H1 detector. The detector components shown are: the electromagnetic (El
hadronic (HAC) and backward electromagnetic (BEMC) calorimeters, forward
and central (CT) trackers, backward proportional chamber (BPC), and scintillato
doscope (TOF).

- The tracker: the central tracking detector consists of two large jet drift chamber modules, two z drift chambers and two multiwire proportional chambers for triggering. Its angular acceptance is $15^0 - 170^0$. The forward tracking detector accepts tracks between 7^0 and 25^0. It consists of three modules of drift and multiwire proportional chambers. The backward multiwire proportional chamber (BPC) has 4 wire planes and an angular acceptance of $155^0 - 175^0$. A superconducting coil provides a uniform magnetic field of 1.2 T in the tracking region.

- The calorimeters: the backward electromagnetic calorimeter (BEMC) is made of 88 lead/scintillator sandwich stacks, each with a depth of 22 radiation lengths, corresponding to about 0.7 interaction lengths, and transverse dimensions of 16 by 16 cm^2. The liquid argon calorimeter consists of an electromagnetic section with lead absorber (20 to 30 radiation lengths) and a hadronic section with steel absorber. The total depth of the calorimeter varies between 4.5 and 8 interaction lengths.

- The time of flight (TOF) system, located behind the backward calorimeter, consists of two scintillator planes, each with a time resolution of about 3 ns, and enables the separation of genuine ep events from proton beam-wall and beam-gas interactions upstream of the detector at the trigger level.

- The luminosity detector system described in [8], not visible in Fig. 1, is designed to detect the $e-\gamma$ coincidence from the reaction $e+p \rightarrow e+\gamma+p$. The electron tagger is located 33m from the interaction region in the backward or $-z$ direction and detects electrons scattered through angles less than 5 mrad with respect to the electron beam direction. The photon tagger is located at $z = -103$m. Both detectors are TlCl/TlBr crystal calorimeters.

At low values of Q^2 the scattered electron deposits its energy in the backward electromagnetic calorimeter. The scattering angle is determined using the backward proportional chamber and the reconstructed event vertex and, at smaller θ_e, the drift chambers. The angles and energies of hadronic final state particles are measured with the central and forward tracking systems and with the liquid argon and backward calorimeters. The analysis in this paper is restricted to electrons detected in the backward calorimeter.

3 Calibration and Resolution

The energy resolution of the BEMC due to sampling fluctuations is $10\%/\sqrt{E}$, as has been determined in test beam studies [9]. The average noise per stack was measured to be 150 MeV which implies that the noise contribution to the measurement of a typical scattered electron shower is about 450 MeV. The measured energy has to be corrected for energy loss in the material in front of the BEMC (about 1 X_o), losses in the wavelength shifter regions between the stacks and for leakage. Monte Carlo simulations showed that all these effects combined give a 2.7% energy correction on average with a fluctuation of $\pm 1.2\%$ due to inhomogeneities. The energy resolution is further affected by stack to stack intercalibration uncertainties which are estimated to be 3.7%. From these considerations the following energy resolution was derived:

$\sigma_E/E = \sigma_{noise}/E \oplus \sigma_{sampling}/\sqrt{E} \oplus \sigma_{const}$, where $\sigma_{noise} = 0.45$ GeV, σ_{sam} $\mathrm{GeV}^{1/2}$, $\sigma_{const} = 0.04$ and E is measured in GeV. This results in a width of the kinematic peak, due to the intrinsic width and detector effects, of about 2.2 (agrees with the observed width.

In the kinematic peak region ($E > 22$ GeV) a χ^2 comparison of the obser spectrum with the Monte Carlo prediction was used to determine the over energy calibration. An additional check was performed by deriving the scatter energy from the angles θ_e of the electron and θ_h of the momentum vector of th system. The energy calibration has an uncertainty of 2%. For the determin from the hadronic final state a combination of well measured tracks in the cen with energy deposits in the calorimeter was used. The calibration of the li calorimeter is presently known to 2% for the electromagnetic and to 7% for th energies[10].

For angles between 174^0 and about 170^0, the electron scattering angle θ mined by the vertex of the event and the reconstructed hit in the BPC. Eve y which contribute to the energy distribution in the kinematic peak may leav in the detector. These are included in the electron energy spectrum but not and x distributions. For smaller angles ($< 170^0$), θ_e can be reconstructed fi in the central chambers. The angular resolution $\delta\theta_e$ depends only weakly o about 6 mrad for interactions with a reconstructed vertex.

The four-momentum transfer squared is determined from the energy and a scattered electron. With the exception of extremely large polar angles, the $\delta Q^2/Q^2$ is dominated by the electron energy resolution and is about 6%. An calculation of Q^2 using the two scattering angles θ_e and θ_h has a similar reso sentially independent of Q^2, and was used as a consistency check. For the dete of $x = Q^2/(sy)$ it is advantageous to combine leptonic and hadronic measu y. The resolution $\delta y_e/y_e$ varies like $1/y$ and is 5% at $y = 0.6$ but deteriorat for $y = 0.1$. The y_h resolution is better than about 30% for $y_h > 0.025$. $y_e < 0.1$, y_h was used in preference to y_e. The resulting x resolution varies be at $x = 10^{-4}$ and 35% at $x = 10^{-2}$. For $x > 10^{-2}$ and small Q^2 hadrons are forward beam pipe region and x measurements are subject to systematic sh will require detailed study in future high statistics analyses.

4 Event Selection and Background

The data presented here correspond to a total integrated luminosity of 1.3 nb is known to a precision of 7%. The trigger pertinent to this analysis requi local energy deposit, or cluster, of more than 4 GeV be identified in the BEM were rejected if signals in both TOF planes were compatible with particles in upstream proton background interactions. The acceptance of this trigger from 90% to 99% for electron energies between 5 and 10 GeV and was larger for electron energies above this. The total number of such triggers recorded $6 \cdot 10^4$.

Deep inelastic scattering event candidates were identified using the followi

- A cluster of more than 6 GeV was required in the backward calorimeter in association with at least one hit in the adjacent BPC. The radial separation of the centre of gravity of the cluster and the BPC hit was required to be less than 15 cm. Furthermore, the cluster centre of gravity had to lie outside the range $|x|$ or $|y| > 16$ cm around the beam axis.

- For events with a BEMC cluster energy below the kinematic peak region (E_e <22 GeV) it was required that at least one track in the central tracker originate from the transverse beam position. The z coordinate of the vertex had to be within ± 50 cm of the nominal interaction point, compatible with the width of the z-vertex distribution of 40 cm (FWHM).

- Out of time proton beam background was further suppressed by restrictive cuts on the signals from the individual TOF scintillator planes.

The resulting sample of 219 events was scanned for remaining beam background and cosmic events, which were removed. The sample of DIS candidates surviving all selection criteria comprised 182 events. In this sample six events were observed with a clear electron tagger signal in coincidence with an energy deposit in the BEMC of less than 10 GeV. These are events where the scattered electron disappears in the beampipe, but hadrons and photons produced in the backward region simulate an electron signal in the BEMC. This implies that the DIS sample contained about 20 to 40 photoproduction events at this stage of the selection procedure. Further evidence for the presence of this background was provided by a comparison of the hadron and the electron y measurements, shown in Fig. 2a. A clear correlation between y_e and y_h is evident in the region in which the y_e resolution is good, $y_e > 0.1$; yet, independent of y_h, there is also an accumulation of events at high y_e, i.e. low electron energies. Fig. 2b shows a Monte Carlo calculation of y_h and y_e, based on the Vector Dominance Model (VDM)[11] for photoproduction. As in the data an accumulation of events at high y_e is seen. Detailed Monte Carlo studies of the photoproduction background using various event generators [11,12], and resolution considerations, led us to reject events if $y_h < y_e/2$, for $y_e > 0.6$. The resulting event sample contained 148 events, none of which had a signal in the electron tagger. The remaining photoproduction contamination could be as much as 50% for $E'_e < 10$ GeV but is estimated to be less than 20% for 10 GeV $< E'_e <$ 14 GeV. For $E'_e > 14$ GeV the photoproduction contamination is negligible. Note that $y = 0.6$ corresponds roughly to $E'_e = 10$ GeV. The lowest x event in this sample has $x = 6 \cdot 10^{-5}$ at $Q^2 = 4$ GeV^2 while the largest[1] Q^2 event has a $Q^2 = 82$ GeV^2 at $x = 4 \cdot 10^{-3}$.

The contamination of the DIS sample with proton and electron beam induced background was estimated to be less than 5% for $E'_e > 10$ GeV, based on studies of the multiplicity of identified low momentum protons and of studies of e and p bunches which have no partner to collide with. Another potential background comes from event pile-up. Due to the high HERA bunch crossing rate of 10 MHz the detector information for an interaction can be distorted by signals resulting from a collision in adjacent bunch crossings. The number of events affected by pile-up was estimated to be less than 1%.

[1] In the same data taking period 5 neutral currents events were detected in the liquid argon calorimeter with $Q^2 > 100$ GeV^2.

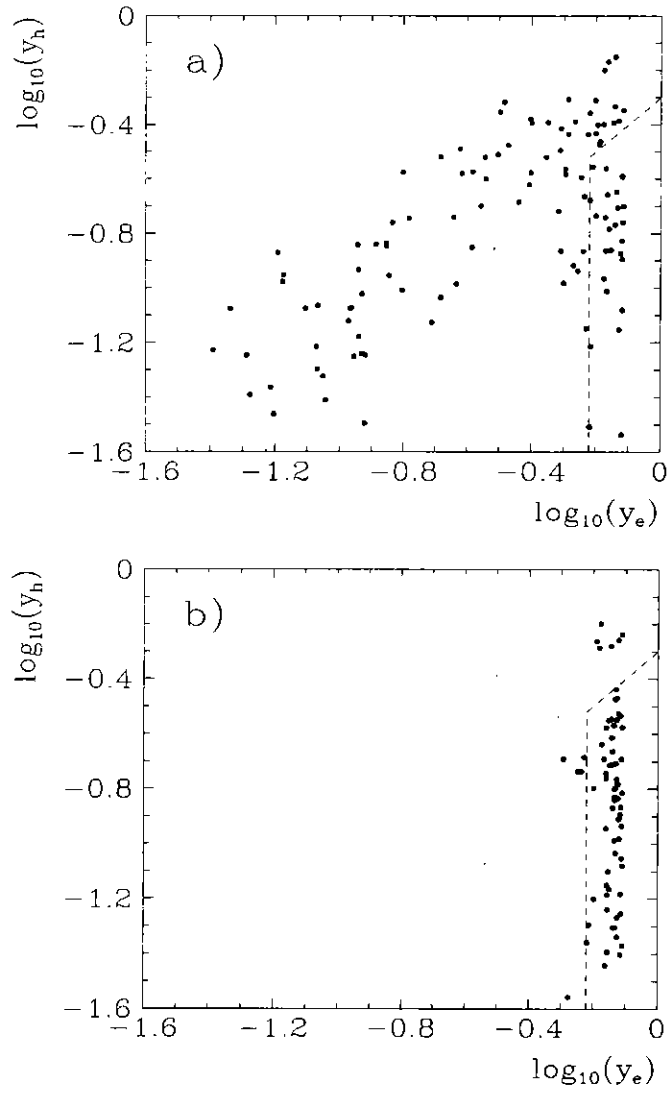

Figure 2: Distribution of $\log_{10} y_e$ versus $\log_{10} y_h$ for (a) DIS candidates and (
lated background events based on the VDM photoproduction event generator
simulated statistics corresponds to 2.5 nb^{-1}. The dashed lines mark the regior
cut which was used to remove photoproduction background.

The energy spectrum of the scattered electron for the accepted data sample is shown in Fig. 3. The expected peak of the distribution at $E'_e = E_e$ is clearly visible. The measured spectrum is compared with a Monte Carlo calculation including a full simulation of the H1 detector. The events have been generated using HERACLES 3.1 [13] for the electroweak interaction, which includes first order radiative corrections, followed by LEPTO 5.2 [14] for the simulation of QCD processes. We chose to represent the parton distributions using the MRSD0 parametrization described in[15].

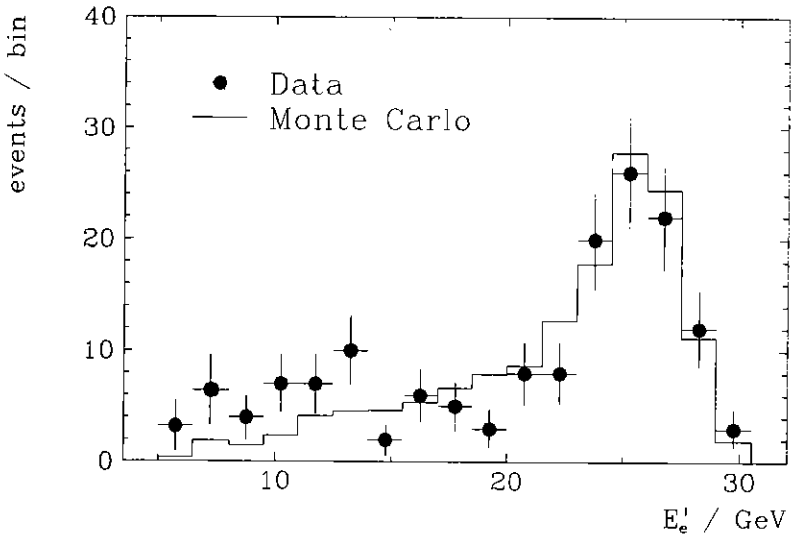

Figure 3: Electron energy spectrum of the DIS events compared with a Monte Carlo simulation [13,14] of the H1 detector using the parametrization MRSD0 [15]. The simulated spectrum is normalized to the measured integrated luminosity of 1.3 nb^{-1}.

The simulated distribution in Fig. 3 was normalized to the measured luminosity. Between 12 and 30 GeV the spectra agree well with a χ^2 of 7.2 for 8 degrees of freedom. The data contain more events in the low energy region than is predicted by the Monte Carlo calculation. This may be due to remaining photoproduction contamination and a low x behaviour of the proton structure functions which is different from that of the MRSD0 parametrization.

5 Differential Cross Sections

In the Born approximation the deep inelastic scattering cross section at low
termined by the two structure functions F_2 and $2xF_1 = F_2/(1+R)$:

$$\frac{d^2\sigma}{dxdQ^2} = \frac{2\pi\alpha^2}{Q^4x}(2\,(1-y)\;+\;\frac{y^2}{1+R})F_2(x,Q^2).$$

In order to reduce sensitivity to the photoproduction background and to the
radiative corrections [16,17] the cross section analysis was limited to $y < 0$
discussed above, a lower y limit was set at $y = 0.025$, ensuring that the y resolu
always better than 30%. In addition it was demanded that $Q^2 > 5\text{GeV}^2$, $\theta_e <$
that the ep interaction vertex be reconstructed, thus reducing the sample to 7
The rejected events are primarily at high E'_e where for kinematic reasons hac
produced with small angles.

The observed distributions were normalized to the measured luminosity
verted into differential cross sections by correcting for the acceptance and finite
effects. The average total acceptance corrections varied between 30% and 50%
ing smearing of the distributions due to finite detector resolution and recon
inefficiencies determined from the data. The cross sections $d\sigma/d\log(x)$ and $d\sigma$
shown in Fig. 4. The $\log(x)$ representation was chosen in order to remove the tr
dependence of the cross section (eq. (3)). The full error bars correspond to the s
error which is the dominating uncertainty. The systematic errors are shown se
All points are subject to a common additional uncertainty of 7% due to the lu
measurement error. In the accessed kinematic range the measured deep inelas
section, not corrected for radiative effects, amounts to $\sigma = (92 \pm 11(stat) \pm 1$
nb.

The calculation of the systematic uncertainty included the following error
possible shifts of the energy scale by 2% and of θ_e by 3 mrad; uncertaintie
trigger (2%) and detector (4%) efficiency calculations; electron and proton beam
background (5%); photoproduction contamination in both the lowest x and
(15%); the influence of different structure functions and hadronization unce
on the acceptance calculation (12% at low x) and the bin size correction (5
statistical error of the Monte Carlo calculation at the largest Q^2 (5% at most)

Fig.4 shows calculations of the cross section for the quark-distribution para
tions MTB1, MTB2[18] and MRSD0, MRSD−[15], using the program [13,14
$R = 0$ is assumed for eq. 3. Note that the parametrizations[15] were obtained fr
including the recent NMC measurements [3] which extend to $x = 0.008$ at $Q^2 =$
The parametrizations differ in their assumptions on the extrapolation of the qu
gluon densities at lower x. Neither data nor firm theoretical predictions [19] a
able in this kinematic region. The MTB2 and MRSD− distributions assume
growth of the parton densities with decreasing x, while MTB1 and MRSD0
a more moderate growth. In the kinematic range of our measurements the r
cross sections calculated with the generated Monte Carlo events are 153 and 12

[2]Note that the y_h - y_e cut was applied only for $y_e > 0.6$. Thus it served only to remove ba
in the lower part of the energy distribution and has no effect on the x, Q^2 distributions.

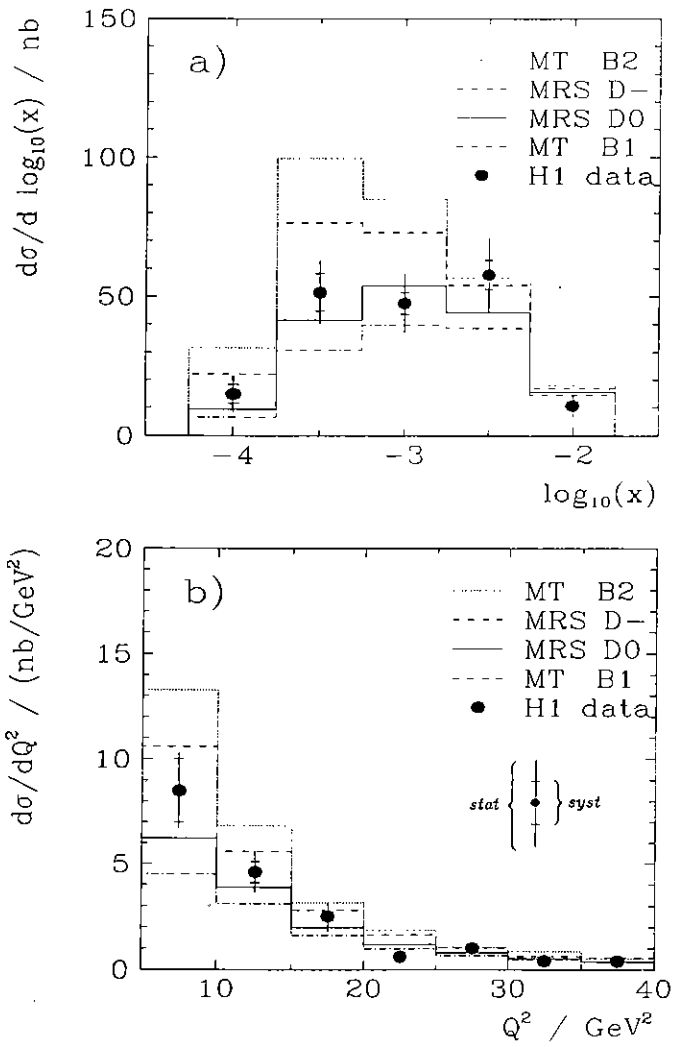

Figure 4: Differential cross sections a) $d\sigma/d\log_{10}(x)$ and b) $d\sigma/dQ^2$ in the range $0.6 > y > 0.025$ and for $Q^2 > 5$ GeV^2 and $\theta_e < 174^0$. The full lines show the results of the cross section calculations [13,14] for different parton density parametrizations. The cross sections are not corrected for radiative effects. The full error bars correspond to the statistical errors; the smaller systematic errors are also indicated.

MTB2 and MRSD− and 69 and 88 nb for MTB1 and MRSD0 respectively. Th calculations agree within 2 standard deviations with our measurement, except made with MTB2, which is more than 3 standard deviations larger.

Neither the Monte Carlo cross sections nor the data are corrected for radiative These have been calculated [17] and are expected to change the cross sections b 40% at the lowest x and Q^2 values. They are an order of magnitude smalle largest x and Q^2 values. The derivation of the Born cross sections, and of F_2, fi measured cross sections requires an iterative procedure, which is left to future a with higher statistics.

6 Conclusions

Deep inelastic scattering has been observed for the first time in a kinematic regi extends down to $x = 10^{-4}$ for Q^2 above 5 GeV^2. The data presented here ste the first luminosity period at HERA, with collisions of 26.7 GeV electrons on 8 protons. The spectrum of the scattered electron energy has been measured d $E'_e = 6$ GeV. It exhibits the predicted peak around the electron beam energy rather flat at smaller energies. The simultaneous measurement of the inclusive r kinematics using the scattered lepton and the hadronic energy and angles ha shown to be an effective means of reducing the large photoproduction backgr low scattered electron energies. This also extends the range of y which can be acc measured to lower y. A measurement of the x and the Q^2 dependent cross section range $Q^2 > 5$ GeV^2, $0.6 > y > 0.025$ and $\theta_e < 174^0$ gives $\sigma = (92 \pm 11(stat) \pm 12$ nb.

Acknowledgements

We are grateful to the HERA machine group whose outstanding efforts made t periment possible. We appreciate the immense effort of the engineers and tech who constructed and maintained the detector. We thank the funding agencies nancial support. We acknowledge the support of the DESY computer center non-DESY members of the collaboration also wish to thank the DESY director the hospitality extended to them.

References

[1] M. Breidenbach et al., Phys.Rev.Lett. 23 (1969) 935.

[2] J. Feltesse, Proceedings of the Lepton Photon Conference 1989, SLAC, Riordan, (1989) 13 and references therein.

[3] P. Amaudruz et al., NMC Collaboration, CERN PPE-92-124, to app Phys.Lett.B.

[4] F. Eisele, *First Results from the H1 Experiment at HERA*, and F. Brasse, *The H1 Detector at HERA*, To appear in: Proceedings of the 26th International Conference on High Energy Physics, Dallas (1992) and DESY preprint 92-140 (1992).

[5] *The H1 Detector at HERA*, H1 Collaboration, *to be submitted to Nuclear Instruments & Methods.*

[6] B. Löhr, *First Results from the ZEUS Experiment at HERA*, To appear in: Proceedings of the 26th International Conference on High Energy Physics, Dallas (1992).

[7] A. Blondel and F. Jacquet, Proc. "An *ep* Facility for Europe", ed. U. Amaldi, DESY 79/48 (1979) 391.

[8] T. Ahmed et al., *Total Photoproduction Cross Section Measurement at HERA Energies*, H1 Collaboration, DESY preprint 92-160, *submitted to Phys. Lett. B.*

[9] *The Backward Electromagnetic Calorimeter in H1, to be submitted to Nuclear Instruments & Methods.*

[10] T. Ahmed et al. *Measurement of the Hadronic Final State in Deep Inelastic Scattering at HERA*, H1 Collaboration, DESY preprint 92-162, *submitted to Phys.Lett.B.*

[11] H1 interface program to LUCVDM of the LUCIFER package of G. Ingelman and A. Weigend (see DESY 87-018), Computer Phys. Comm. 46 (1987) 241.

[12] T. Sjöstrand, PYTHIA at HERA, Proc. Workshop "Physics at HERA", eds. W. Buchmüller and G. Ingelman, Hamburg, 3, (1991) 1405.

[13] A. Kwiatkowski, H. Spiesberger, and H.-J. Möhring, Comp. Phys. Commun. 69(1992) 155, and references therein.

[14] G. Ingelman, "LEPTO 5.2", unpublished program manual;
H.Bengtsson, G.Ingelman, and T.Sjöstrand, Nucl. Phys. B301 (1988) 554.

[15] A. D. Martin, W. J. Stirling, R. G. Roberts, Durham preprint, DTP-92-16 (1992).

[16] H. Spiesberger et al., Proc. Workshop "Physics at HERA", eds. W. Buchmüller and G. Ingelman, Hamburg, 3, (1991) 798.

[17] A. Akhundov et al., Proc. Workshop "Physics at HERA", eds. W. Buchmüller and G. Ingelman, Hamburg, 3, (1991) 1285;
A. Akhundov et al., private communication.

[18] J. Morfin and W. K. Tung, Z. Phys. C52 (1991) 13 (The parton density parametrizations in the DIS scheme were used).

[19] L. V. Gribov, E. M. Levin and M. G. Ryskin, Nucl. Phys. B188 (1981) 555; Phys. Rep. 100 (1983);
A. H. Mueller and J. Qiu, Nucl. Phys. B268 (1986) 427.